Involvement of NLRP3-inflammasome pathway in noise-induced hearing loss

Na Sai[1, 2, 3, 4, #], Yuan-Yuan Yang[5, #], Long Ma[6], Da Liu[1, 2, 3, 4], Qing-Qing Jiang[1, 2, 3, 4], Wei-Wei Guo[1, 2, 3, 4, *], Wei-Ju Han[1, 2, 3, 4, *]

From the Contents

Graphical Abstract *Activation of NLRP3-inflammasome is an important pathological mechanism involved in the development of noise-induced hearing loss in miniature pigs*
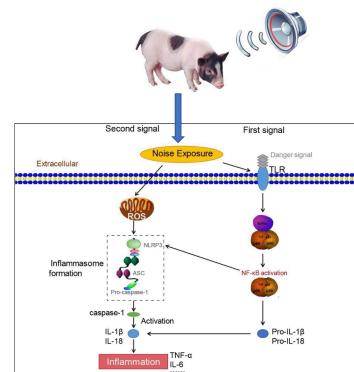
Abstract

The inflammasome is a multiprotein oligomer in the cell cytoplasm and is part of the innate immune system. It plays a crucial role in the pathological process of noise-induced hearing loss (NIHL). However, the mechanisms of NLR family pyrin domain containing 3 (NLRP3) inflammasome activation in NIHL have not been clearly demonstrated. In this study, miniature pigs were exposed to white noise at 120 dB(A) and auditory brainstem response measurements were used to measure their hearing function. Immunofluorescence staining, confocal laser scanning microscopy, western blot assay, and quantitative reverse transcription-polymerase chain reaction were used to analyze inflammasome-related protein distribution and expression. NLRP3, interleukin-1β, interleukin-18, and cleaved-caspase-1 were highly expressed in the cochlea after 120 dB(A) white noise exposure. Our findings suggest that NLRP3-inflammasomes in the cochlea may be activated after acoustic trauma, which may be an important mechanism of noise-induced hearing loss.
Key Words: acoustic injury; inflammasome; interleukin-1β; miniature pig; NLR family pyrin domain containing 3 (NLRP3); noise-induced hearing loss; sensorineural hearing loss

Introduction

Sensorineural hearing loss (SNHL) is an increasingly common problem in the world, and noise-induced hearing loss (NIHL) is the second most common cause of nonhereditary hearing impairment (Kurabi et al., 2017; Zheng and Zuo, 2017). It has been suggested that more than 600 million people worldwide live with NIHL (Le et al., 2017).

Studies have shown that acoustic injury of the auditory system can be caused by multiple factors, including mechanical damage of hair cells, microcirculation vascular damage, and metabolic disorders that lead to hair cell death (Cai et al., 2014; Zheng and Zuo, 2017; Wang and Puel, 2018). Several recent studies have reported that the immunological and inflammatory responses to acoustic overstimulation in the cochlea play a crucial role in the development of NIHL (Cai et al., 2014; Vethanayagam et al., 2016; Yang et al., 2016; Frye et al., 2019). Previously, we reported an increase of reactive oxygen species (ROS) and nuclear factor kappa-B (NF-κB p65) nuclear translocation during the acute hearing loss stage in miniature pig inner ear hair cells following acoustic trauma (Sai et al., 2020).

The inflammasome is a multiprotein oligomer and part of the innate immune system. Its primary components include pattern recognition receptors (PRRs), apoptosis-associated speck-like protein containing CARD (ASC), and procaspase-1 (Martinon et al., 2002). Researchers have identified a number of PRRs involved in inflammasomes, including NOD-like receptors (NLRs) family pyrin domain, such as NLRP1, NLRP3, NLRP6, NLRP7, and NLRP12, CARD domain containing 4 (NLRC4), absence in melanoma 2 (AIM2), IFI16, and RIG-I (Schroder and Tschopp, 2010). Inflammasomes form in response to a wide range of pathogen- or danger-associated molecular patterns (PAMPs or DAMPs). Through the self-cleavage of procaspase-1, the inflammasome activates caspase-1, which causes the maturation of interleukins 1β and 18 (IL-1β and IL-18) (Malik and Kanneganti, 2017). IL-1β and IL-18 are released extracellularly for participation in inflammation, injury, and other processes (Gross et al., 2011). Several recent investigations have shown that SNHL is linked to inflammasome activation (Martinon et al., 2009; Kuemmerle-Deschner et al., 2015; Shi et al., 2015, 2017; Zhuang et al., 2018). Nevertheless, the data indicating that inflammasomes have a role in NIHL development are limited. The aim of this study was to explore the involvement of the NLRP3-inflammasome pathway in the regulation of noise-induced cochlear injury.

Materials and Methods

Animals
Twenty healthy miniature pigs (2–3 months old, weighing 5–6 kg) were

[1]College of Otolaryngology Head and Neck Surgery, Chinese PLA General Hospital, Beijing, China; [2]National Clinical Research Center for Otolaryngologic Diseases, Beijing, China; [3]Key Laboratory of Hearing Science, Ministry of Education, Beijing, China; [4]Beijing Key Laboratory of Hearing Impairment for Prevention and Treatment, Beijing, China; [5]Department of Otolaryngology Head and Neck Surgery, Peking University Shenzhen Hospital, Shenzhen, Guangdong Province, China; [6]PLA Rocket Force Characteristic Medical Center Department of Stomatology, China
*Correspondence to: Wei-Wei Guo, MD, gwent001@163.com; Wei-Ju Han, MD, PhD, hanweiju@aliyun.com.
https://orcid.org/0000-0002-2001-7956 (Wei-Wei Guo); https://orcid.org/0000-0002-8739-481X (Wei-Ju Han)
#These authors contributed equally to this work.

purchased from Zhuozhou Kangning Miniature Pig Cultivation Company (Hebei, China, license No. SYXK (Ji) 018-003). To avoid the effects of individual differences on the study results, only male pigs were used in this study, and a baseline hearing test using auditory brainstem response (ABR)-click was performed on all animals. There were ten pigs in the normal control group and ten pigs in the noise exposure group. Following the baseline hearing test, animals were randomly allocated to either the noise exposure or normal control group (using a random number table). All animals were subjected to a 12-hour light/dark cycle and had access to food and water *ad libitum*. Procedures involving the use and care of animals were approved by the Institutional Animal Care and Use Committee of Chinese PLA General Hospital on March 6, 2017 (approval No. 201709) and were conducted in strict accordance with international laws and National Institutes of Health (NIH) policies, including the Guide for the Care and Use of Laboratory Animals (8th ed, 2011). This study was reported in accordance with the ARRIVE 2.0 guidelines (Animal Research: Reporting of *In Vivo* Experiments) (Percie du Sert et al., 2020).

Noise exposure
The animals in the noise exposure group were placed in a wire mesh cage and subjected to 3 hours of white noise at 120 dB(A) for 2 consecutive days. The control group did not receive noise treatment. The noise signal was generated using a signal processor (RZ6, Tucker Davis Technologies [TDT], Alachua, FL, USA). The signal was routed through an attenuator (PA5, TDT) and an amplifier (Crown, XLS402, Pittsburgh, PA, USA) to a loudspeaker (Zhenmei Co., Ltd., Jiangsu, China), which was placed 20 cm above the animal's head. This noise exposure regimen resulted in a permanent loss of cochlear sensitivity as described in our previous research (Wu et al., 2017; Sai et al., 2020).

Auditory brainstem response testing
To assess hearing function, we measured ABR before and one day after noise exposure. In brief, an animal was put in a sound-proof chamber after being sedated with an intramuscular injection of xylazine hydrochloride (0.1 mL/kg; Shengda Reagent Co., Ltd., Jilin, China) and under anesthesia with 3% pentobarbital sodium (1 mL/kg, intramuscular injection; Sigma, St. Louis, MO, USA). The same method of anesthesia was used in all experiments in this study. A warming blanket was used to keep the body temperature at 38°C. Subdermal stainless-steel needle electrodes were inserted at the vertex (noninverting input) and behind the stimulated and non-stimulated ears (inverting input and ground, respectively). An open-field sound delivery device positioned 1 cm from the animal's tested ear was used to stimulate each ear independently. Clicks and tone bursts at 2, 4, 8, 16, and 24 kHz were used to elicit ABRs, which were produced digitally (SigGen, TDT) with a multifunction processor (MEDUSA4Z, TDT). The procedures and parameter settings were similar to those used in previous reports (Hu et al., 2012; Wu et al., 2017). The ABR threshold was established as the weakest stimulus intensity that dependably generated a detectable signal.

Cochlear tissue collection
After the ABR tests, cochleae were removed for gene expression and pathological examination of each group. The animals were heavily anesthetized with pentobarbital sodium and then decapitated. As previously reported, the cochleae were rapidly detached from the skull (Chen et al., 2016). The cochleae were perfused with an RNA stabilization reagent (RNAlater; Thermo Fisher Scientific, Waltham, MA, USA) to examine the transcriptional expression patterns of the NLRP3-inflammasome and related genes of inflammatory factors. The cochleae were promptly frozen in liquid nitrogen for 10 minutes after being washed with 0.01 M phosphate-buffered saline (PBS) before being kept at –80°C for western blot analysis. The cochleae were preserved in 4% paraformaldehyde overnight at 4°C for immunohistological and pathological investigations. The organ of Corti and stria vascularis were harvested after the dissection of the cochleae in PBS for immunofluorescent staining.

Immunofluorescence staining
We used immunofluorescence staining to observe the immunoreactivity of caspase-1 and IL-1β in the cochleae. Tissue processing and immunofluorescence of the cochleae were performed as previously reported (Wu et al., 2017; Sai et al., 2020). After the organ of Corti and stria vascularis were recovered, the tissues were permeabilized for 15 minutes in PBS with 0.25% Triton X-100, blocked for 30 minutes in PBS with 5% goat serum, and incubated overnight at 4°C with the appropriate primary antibody (caspase-1: rabbit, 1:100, Abcam, Cambridge, MA, USA, ab-1872, RRID: AB_302644; IL-1β: rabbit, 1:100, Abcam, ab-104279, RRID: AB_10711147; NF200: mouse, 1:200, Abcam, ab-82259, RRID: AB_1658500). After that, the tissues were washed three times with PBS and treated with a secondary antibody (Alexa Fluor 488-labeled donkey anti-rabbit antibody for caspase-1 and IL-1β, 1:200, Invitrogen, Carlsbad, USA, A10011; Alexa Fluor 568-labeled goat anti-mouse antibody for NF200, 1:200, Invitrogen, A11011) for 1 hour at room temperature, and for 10 minutes with a propidium iodide (Sigma, P4170) or DAPI (Abcam, ab228549) counterstain (5 μg/mL in PBS).

Six cochleae were stained for caspase-1 and IL-1β in the noise exposure group. The normal control group included cochleae from three more animals (six cochleae) that were not subjected to noise exposure. To test nonspecific staining, several pieces of tissue from these cochleae were stained exclusively with the secondary antibodies.

We observed the fluorescence using a confocal microscope (Zeiss, LSM780

laser scanning confocal imaging system, Heidelberg, Germany). The number of immunoreactive hair cells was counted for quantitative investigation as described previously (Hu et al., 2012). The cells with malformed nuclei (condensed, fragmented, or swollen) were considered damaged cells. The numbers of damaged and missing hair cells and spiral ganglion cells were quantified for each cochlea based on the nuclear morphology (Chen et al., 2018). The average numbers for each experimental condition were assembled into a graph showing the frequency-place correlation for each pig.

Western blot assay
Western blotting was carried out to detect the expression of inflammasome-related proteins. Eight cochleae were used from each group. RIPA was used to lyse pig cochleae tissues. The tissue samples were homogenized using the Tissue Protein Extraction Kit (CW0891; Beijing Kangwei Biotechnology Co., Ltd., Beijing, China). Afterwards, the homogenates were centrifuged at 12,000 × *g* for 10 minutes at 4°C. The total amount of protein in each supernatant fraction was determined using the Bio-Rad DC protein assay, and an aliquot of each supernatant was removed and stored at −80°C. Equal amounts of total supernatant protein in loading buffer were boiled for 5 minutes, and then separated on a 10% sodium dodecyl sulfate/polyacrylamide gel. Briefly, proteins sorted in an SDS-PAGE gel were transferred to a polyvinylidene fluoride membrane (Millipore, Bedford, MA, USA). Subsequently, each blot underwent immunoreaction with anti-IL-6 (rabbit, 1:100, Abcam, Cat# ab7737, RRID: AB_306031), anti-NF-κB p65 (rabbit, 1:50, Cell Signaling Technology, Danvers, MA, USA, Cat# 3034, RRID: AB_330561), anti-IL-18 (rabbit, 1:100, Abcam, Cat# ab71495, RRID: AB_1209302), anti-IL-1β (rabbit, 1:100, Abcam, Cat# ab104279, RRID: AB_10711147), anti-tumor necrosis factor-α (TNF-α; rabbit, 1:100, Abcam, Cat# ab6671, RRID: AB_305641), anti-Caspase-1 (a polyclonal antibody that stains both procasp-1 and cleaved casp-1; rabbit, 1:100, Abcam, Cat# ab1872, RRID: AB_302644), and anti-NLRP3 (rabbit, 1:100, Abcam, Cat# ab-91413, RRID: AB_2049514) antibodies and anti-β-actin (mouse, 1:100, Abcam, Cat# ab8226, RRID: AB_306371). Then, they were incubated with secondary antibodies (goat anti-mouse IgG (H+L), horseradish peroxidase-conjugated, 1:1000, TDY Biotech Co., Ltd., Beijing, China, Cat# S001; goat anti-rabbit IgG (H+L), horseradish peroxidase-conjugated, 1:1000, TDY Biotech Co., Ltd., Cat# S004). Protein bands were detected using the chemiluminescence substrate (32109, ECL Plus; Amersham Biosciences, Piscataway, NJ, USA) after each antibody preparation was diluted in 5% skim milk (WBKLS0500, Millipore). The intensities of the protein bands were quantified using ImageJ software (National Institutes of Health, Bethesda, MD, USA; Schneider et al., 2012). Protein expression was normalized to β-actin.

Quantitative reverse transcription-polymerase chain reaction
Total RNA from each pig's cochleae was separately extracted with RNeasy (Qiagen, Venlo, Netherlands). Each group of four pigs (eight cochleae) was analyzed for *NLRP3*, *Caspase-1*, *IL-1β*, *IL-18*, *NF-κB p65*, *IL-6*, *TNF-α* and *GAPDH* mRNA with quantitative reverse transcription-polymerase chain reaction (RT-PCR). Complementary DNA (cDNA) was synthesized from 5 μg total RNA using the SuperScript III Reverse Transcriptase (Thermo Fisher Scientific). PCR amplification of the cDNA and quantification was performed using SYBR (Thermo Fisher Scientific). The PCR conditions were as follows: holding stage for 1 denaturation cycle at 95°C for 20 seconds, cycling stage for 40 denaturation cycles at 95°C for 3 seconds and annealing at 59°C for 30 seconds. GAPDH as an internal standard was arbitrarily assigned a value of 1.0. The $2^{-\Delta\Delta CT}$ method was used to analyze the relative product levels of quantitative RT-PCR gene expression (Zhang et al., 2013; Zhuang et al., 2018). The sequence-specific primers for quantitative RT-PCR were shown in **Table 1**.

Table 1 │ The sequences of primers

Gene	Primer sequence (5'–3')	Product size (bp)
NLRP3	F: GAC CTC AGC CAA GAT GCA AG	168
	R: TCT GAT GCC CAG TCC AAC AT	
Caspase-1	F: CCT CGA ACT CTC CAC AGG TT	123
	R: GAA GAC GCA GGC TTA ACT GG	
NF-κB p65	F: TGC ATC CAC AGC TTC CAG AAC	149
	R: CGC ACA GCA TTC AGG TCG TA	
IL-1β	F: CAC ACA TGC TGA AGG CTC TC	171
	R: GGG TGG GCG TGT TAT CTT TC	
IL-18	F: CGA TGA AGA CCT GGA ATC GG	159
	R: ACG TCT GGA GGT GCA TTA TCT	
TNF-α	F: AAG TCA ACC TCC TCT CT GC	98
	R: CCT CCC AGG TAG ATG GGT TC	
IL-6	F: ATG GCT ACT GCC TTC CCT AC	65
	R: TCT GAG GTG GCA TCA CCT TT	
GAPDH	F: TGG AAA GGC CAT CAC CAT CT	105
	R: ATG GTC GTG AAG ACA CCA GT	

F: Forward; GAPDH: glyceraldehyde-3-phosphate dehydrogenase; IL: interleukin; NLRP3: NLR family pyrin domain containing 3; NF-κB: nuclear factor kappa-B; R: reverse; TNF-α: tumor necrosis factor-α.

Statistical analysis

No statistical methods were used to predetermine sample sizes; however, our sample sizes are similar to those reported in previous publications (Hu et al., 2012; Wu et al., 2017). The mean ± standard deviation was used to express data. Protein expression, average ABR thresholds, and immunoreactivity for the control and noise exposure groups were compared with Student's *t*-test using SPSS version 19.0 (IBM, Armonk, NY, USA). $P < 0.05$ was considered statistically significant.

Results

Noise exposure causes loss in cochlear sensitivity

The average hearing threshold of the normal control group was 21.5 ± 4.7 dB sound pressure level (SPL), and was 70.5 ± 5.5 dB SPL in the noise exposure group (**Figure 1A**). The threshold shifts were most significant at 4 kHz, and high-frequency hearing loss was more severe than low-frequency hearing loss (**Figure 1B**), which is consistent with acute NIHL-associated human hearing function (Le et al., 2017).

To determine the effect of acoustic trauma on sensory cell loss, specifically hair cells (HCs) and spiral ganglion cells (SGCs), we quantified the number of missing cells in the normal control and noise-exposed (NE) cochleae (**Figure 1C–E**). When compared with the control group, the NE animals had an 85.9% increase in the total number of missing outer hair cells (OHCs), with a statistically significant difference ($P < 0.01$; **Figure 1C** and **D**). The increase in

sensory cell damage caused by excessive noise occurred mostly in the middle and basal portions of the cochlear sensory epithelium (40–100% distance from the apex), which was consistent with the hearing function changes (**Figure 1C**). In addition, the noise exposure group had a significantly lower number of SGCs compared with the control group ($P < 0.05$; **Figure 1E**).

Noise-induced activation of NLRP3-inflammasomes in pig cochlea

The noise exposure group had elevated mRNA and protein levels of cleaved caspase-1 and NLRP3 in the cochleae compared with those in the control group (**Figure 2A–C**). Immunofluorescence (IF) results showed that the increased caspase-1 immunoreactivity was mainly located in SGCs and HCs (**Figure 2D** and **E**), and the noise exposure group had elevated immunoreactivity of caspase-1 in SGCs and HCs compared with those in the normal control group ($P < 0.05$; **Figure 2F**). These results indicate that NLRP3 is involved in inflammasome activation during NIHL. Additionally, mRNA and protein expression of IL-18 and IL-1β were both increased in noise-treated pig cochleae compared with those in the normal control group ($P < 0.01$; **Figure 3A–C**). Immunofluorescence showed that the increased IL-1β immunoreactivity was mainly located in spiral ganglion, hair cells and the stria vascularis (SV) (**Figure 3D–F**).

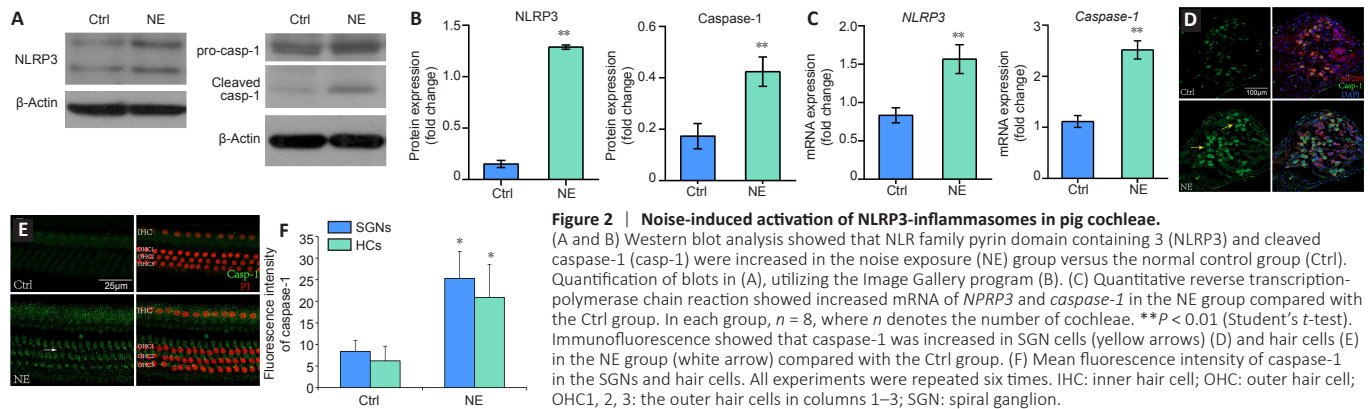### Noise exposure induces increase in inflammatory factors

In the noise exposure group, mRNA and protein levels of activated inflammatory factors IL-6, TNF-α, and NF-κB p65 in the cochleae were significantly increased compared with those in the normal control group (**Figure 4A–C**).
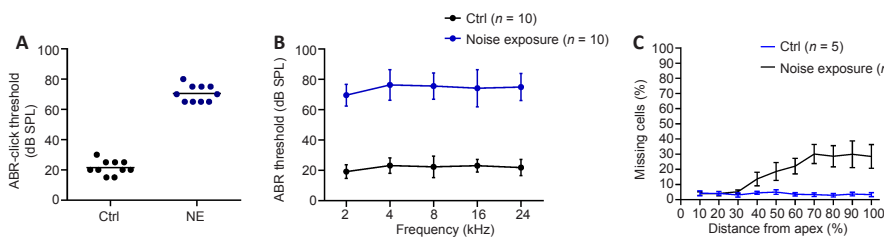

Figure 1 │ Noise-induced cochlear trauma and hearing function changes.
(A, B) Auditory brainstem response (ABR)-click thresholds (A) and ABR tone-burst thresholds (B) in the noise exposure (NE) and normal control (Ctrl) groups. (C) The distance from the apex of the cochlea to the hook process is 0–100% (apex = 0%, base = 100%). Cochleogram distribution of the missing outer hair cells between the two groups in the cochleae. (D) The number of missing outer hair cells (OHCs) per cochlea. (E) Substantial reduction in the number of spiral ganglion cells (SGCs) caused by noise exposure. *$P < 0.05$, **$P < 0.01$, *vs.* ctrl group (Student's *t*-test). $n = 10$ in each group in A and B, $n = 5$ in each group in C–E, where n denotes the number of cochleae. All experiments were repeated six times.


Figure 2 │ Noise-induced activation of NLRP3-inflammasomes in pig cochlea.
(A and B) Western blot analysis showed that NLR family pyrin domain containing 3 (NLRP3) and cleaved caspase-1 (casp-1) were increased in the noise exposure (NE) group versus the normal control group (Ctrl). Quantification of blots in (A), utilizing the Image Gallery program (B). (C) Quantitative reverse transcription-polymerase chain reaction showed increased mRNA of *NPRP3* and *caspase-1* in the NE group compared with the Ctrl group. In each group, $n = 8$, where n denotes the number of cochleae. **$P < 0.01$ (Student's *t*-test). Immunofluorescence showed that caspase-1 was increased in SGN cells (yellow arrows) (D) and hair cells (E) in the NE group (white arrow) compared with the Ctrl group. (F) Mean fluorescence intensity of caspase-1 in the SGNs and hair cells. All experiments were repeated six times. IHC: inner hair cell; OHC: outer hair cell; OHC1, 2, 3: the outer hair cells in columns 1–3; SGN: spiral ganglion.
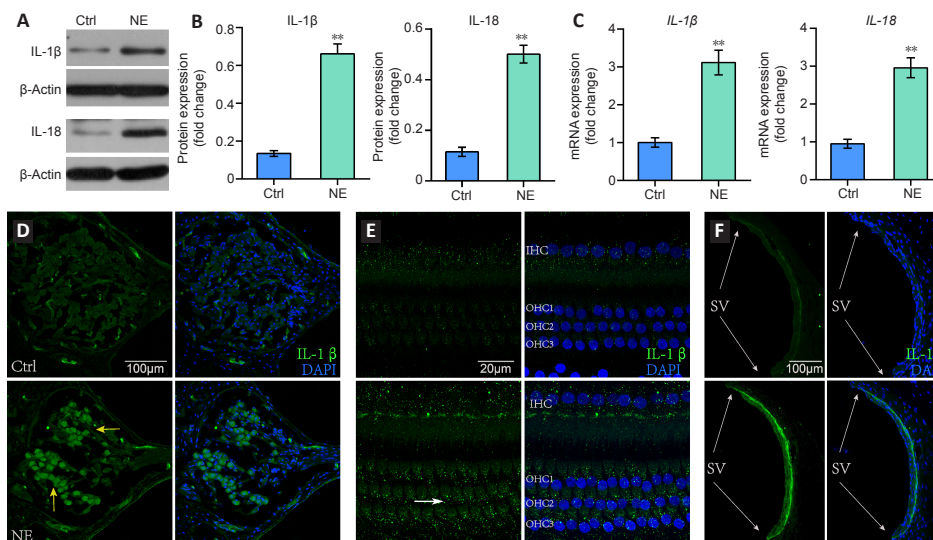
Figure 3 │ IL-18 and IL-1β expression levels increased after cochlear acoustic trauma.
One day after NE, western blot analysis (A) showed that both IL-1β and IL-18 were increased in the noise exposure (NE) group compared with the normal control group (Ctrl). Quantification using Image Gallery software (B) of blots in A. In each group, $n = 8$, where n denotes the number of cochleae. (C) Quantitative reverse transcription-polymerase chain reaction showed increased *IL-1β* and *IL-18* mRNA levels in the NE group compared with those in the Ctrl group. In each group, $n = 8$, where n denotes the number of cochleae. Asterisks indicate a significant difference (**$P < 0.01$). Immunofluorescence showed increased expression of IL-1β in the spiral ganglion cells (yellow arrows) (D), hair cells (white arrow) (E), and the stria vascularis (SV) (gray arrows) (F) after noise exposure. All experiments were repeated six times. IL: Interleukin.
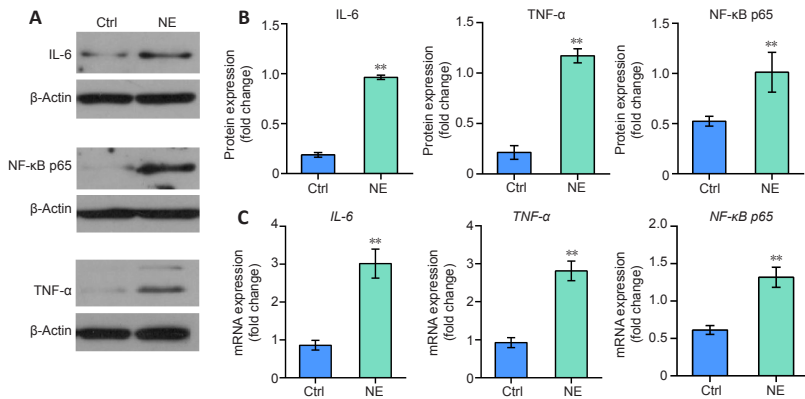
Figure 4 | Inflammatory factors upregulated by cochlear acoustic trauma.
Western blot analysis showed that the inflammatory markers IL-6, TNF-α, and NF-κB p65 were increased in the noise exposure group (NE) compared with those in the normal control group (Ctrl) (A) 1 day after NE. Quantification using the Image Gallery program (B) of blots in (A). In each group, *n* = 8, where *n* denotes the number of cochleae. (C) Quantitative reverse transcription-polymerase chain reaction revealed higher mRNA levels of *NF-κB p65*, *IL-6*, and *TNF-α* in the NE group compared with those in the Ctrl group. In each group, *n* = 8, where *n* denotes the number of cochleae. Asterisks indicate a significant difference (**$P < 0.01$, Student's *t*-test). All experiments were repeated six times. IL: Interleukin; NF-κB: nuclear factor kappa-B; TNF-α: tumor necrosis factor-α.

Discussion

The NLRP3-inflammasome and related inflammatory factors are involved in various cellular processes linked to SNHL (Shi et al., 2015; Nakanishi et al., 2017; Shi et al., 2017; Zhuang et al., 2018; Feng et al., 2020). Here, we provide evidence that the NLRP3-inflammasome pathway is involved in the regulation of noise-induced cochlear injury. Furthermore, our findings suggest that the downstream inflammatory components of the NLRP3-inflammasome could be investigated as potential therapeutic targets in the treatment of noise-induced cochlear dysfunction and sensory cell destruction.

In this study, miniature pigs were exposed to 120 dB(A) white noise to establish the NIHL model. With the exception of other primates, pigs share the closest evolutionary kinship to humans. In particular, the pig inner ear anatomy is similar to the structure of the human inner ear (Yang, 2016; Zhong et al., 2018). After noise stimulation, the most severe hearing loss in pigs occurred at 4 kHz, which is consistent with the affected frequencies in human NIHL. Chen et al. established a model of explosive deafness using 145 dB SPL impulse noise exposure (Chen et al., 2016). In the study, the average hearing threshold raised by more than 70 dB SPL after 50 exposures to impulsive noise, which is substantially greater than the 49 dB SPL difference found between the white noise exposure group and control group in our investigation. This discrepancy suggests that impulse noise may cause more serious inner ear damage. Furthermore, although the structure of the organ of Corti was unaltered in a previous study, the inner and outer hair cells were missing to varying degrees (Chen, 2014). However, there was no evident loss of IHCs in the present study, and only a partial loss of OHCs and SGCs were observed in the noise exposure group cochleae. This suggests that the damage to the cochlea from the impulse noise injury was primarily mechanical, whereas the predominant damage to the cochlea from the 120dB(A) white noise was metabolic.

The inner ear was once thought to be an "immune privileged" organ because of the presence of the blood-labyrinth barrier. However, the inflammatory/immune response has been considered as a key mechanism of NIHL and the primary response of the noise-stimulated cochlea (Vethanayagam et al., 2016; Yang et al., 2016; Hu et al., 2018; Sai et al., 2020). In the present study, acoustic damage activated the NLRP3-inflammasome in pig cochleae. IL-18 and IL-1β mRNA and protein levels were also increased in the HCs, SGCs, and SVs of the noise exposure group compared with those in the control group. The expression of NLRP3 in cells was very low in the control animals. NLRP3-inflammasome activation is thought to require two signals. The first signal, the pre-stimulation signal, interacts with Toll-like receptors (TLRs) and activated NF-κB to increase the expression of NLRP3, pro-IL-18, and pro-IL-1β (Bauernfeind et al., 2009; Zhou et al., 2011). It has been reported that acoustic injury activates immune/inflammatory responses through TLRs signaling pathways (Vethanayagam et al., 2016). The second signal, including PAMPs and DAMPs, is recognized by NLRP3, then ASC is recruited to induce procaspase-1 self-cleavage, and finally, caspase-1 triggers downstream IL-1β and IL-18 activation and release, or induces cell pyroptosis (Bauernfeind et al., 2009; Schroder and Tschopp, 2010; Zhou et al., 2011). We believe that the secondary inflammasome signals produced by acoustic injury are: 1) extracellular ATP stimulation-induced opening of potassium channels, resulting in intracellular K$^+$ reduction and Ca^{2+} inflow (Ayna et al., 2012); 2) lysosomal enzyme release (Eisenbarth and Flavell, 2009; Duewell et al., 2010); and 3) excessive ROS accumulation in cells.

In conjunction with our prior research (Sai et al., 2020), we speculate that excessive ROS buildup is a key element in NLRP3-inflammasome activation. Furthermore, ROS inhibitors or scavengers have been shown to prevent NLRP3-inflammasome activation (Dostert et al., 2008). It has been reported that the proinflammatory cytokine IL-1 increased the number of leukocyte-injured neurons and caused NO, TNF-α, and IL-6 to be secreted from microglia, resulting in neurotoxicity (Frye et al., 2019; Wang et al., 2019). Therefore, the NLRP3-inflammasome and its downstream factors, IL-18 and IL-1β, can further promote the secretion of inflammatory factors such as TNF-α and IL-6. In our study, we also found that NF-κB, TNF-α, and IL-6 were increased in the noise exposure group. TNF-α and IL-6 combine with TLRs to activate the NF-κB signaling pathway to induce apoptosis and necrosis. As a first signal, the latter can activate the inflammasome. The auditory nervous

system is harmed by downstream inflammation and ROS, resulting in NIHL. The pathway mentioned above may form in the cochlea and exacerbate the initial inflammatory response (**Figure 5**).
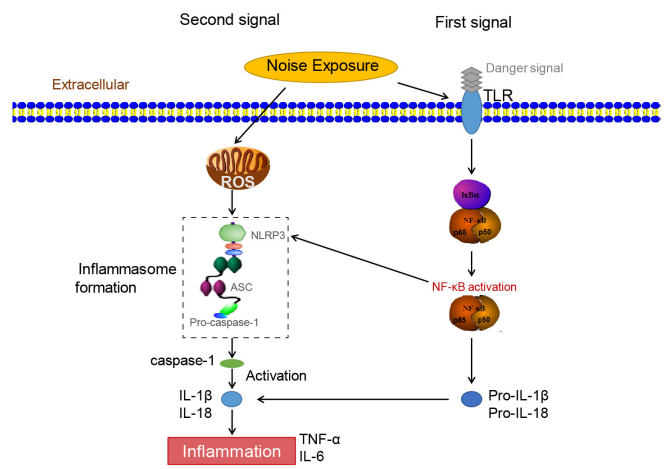
Figure 5 | The possible pathways of NLRP3-inflammasomes involved in NIHL.
The first signal: noise stimulation activates the NF-κB signaling pathway via TLRs, increasing the production of NLRP3, pro-IL-18, and pro-IL-1β. The second signal: the NLRP3-inflammasome, IL-18 and IL-1β are activated by the buildup of ROS caused by acoustic trauma, which further promotes inflammation. ASC: Apoptosis-associated speck-like protein containing CARD; IL: interleukin; NF-κB: nuclear factor kappa-B; ROS: reactive oxygen species; TLR: Toll-like receptors; TNF: tumor necrosis factor.

Under normal conditions, the NLRP3-inflammasome plays a vital role in defending the body from external bacterial and viral infection, and maintaining homeostasis as part of the innate immune response (Martinon et al., 2009). However, if its activation becomes uncontrollable, an excessive inflammatory response occurs, such as NLRP3 gene mutation, which can lead to Muckle-Wells syndrome (MWS), family Mediterranean fever, and other diseases. Previous studies of MWS reported that IL-1β inhibitors improved or stabilized the hearing function of the majority of patients through developing progressive SNHL (Kuemmerle-Deschner et al., 2015; Tran, 2017; Marchica et al., 2018). Furthermore, it has been confirmed that the auditory threshold elevation began primarily at higher frequencies (Koitschev et al., 2012), suggesting that the initial location of pathologic trauma to the inner ear in MWS patients may be in the basal turn of the cochlea, which is consistent with hearing function changes in NIHL (Le et al., 2017). In conclusion, we believe that noise-induced pathogenesis of hearing impairment, like in MWS, appears to be related to excessive activation of the NLRP3-inflammasome, excessive production of IL-1, and downstream inflammation. Thus, we believe that NLRP3-inflammasome inhibitors or interleukin-1 inhibitors have high potential as therapeutic targets for NIHL prophylaxis.

Limitations
This study did not investigate whether attenuation of inflammasome activity or anti-inflammatory therapy would lead to preservation of the ABR threshold or OHC and SGC numbers within this model. We will investigate whether anti-inflammatory or NLRP3-inflammasome-targeted drugs lead to protection of hearing function, OHCs and SGCs in future research.

Conclusion
In this study, a pig model of noise-induced hearing loss was established using 120 dB(A) white noise. White noise mainly caused high-frequency hearing loss at frequencies above 4 kHz. Noise exposure activated the NLRP3-inflammasome in the cochlea, and increased IL-18 and IL-1β production. In addition, the expressions of NF-κB and its downstream inflammatory factors IL-6 and TNF-α were upregulated. The findings suggest that the NLRP3-

inflammasome and its downstream inflammatory factors promote the secretion of inflammatory factors such as TNF-α and IL-6, which activate the NF-κB signaling pathway by combining with TLRs to induce apoptosis and necrosis. The NF-κB signaling pathway could be the first signal to activate the inflammasome and provoke the above-mentioned circulation in the cochlea, which could aggravate the initial inflammatory response and neurotoxicity, and aggravated the cochlear damage. Therefore, inflammasome activation is likely an important molecular mechanism involved in the acoustic damage of the cochlea in miniature pigs, which suggests potential therapeutic targets for NIHL.

References

Ayna G, Krysko DV, Kaczmarek A, Petrovski G, Vandenabeele P, Fésüs L (2012) ATP release from dying autophagic cells and their phagocytosis are crucial for inflammasome activation in macrophages. PLoS One 7:e40069.

Bauernfeind FG, Horvath G, Stutz A, Alnemri ES, MacDonald K, Speert D, Fernandes-Alnemri T, Wu J, Monks BG, Fitzgerald KA, Hornung V, Latz E (2009) Cutting edge: NF-kappaB activating pattern recognition and cytokine receptors license NLRP3 inflammasome activation by regulating NLRP3 expression. J Immunol 183:787-791.

Cai Q, Vethanayagam RR, Yang S, Bard J, Jamison J, Cartwright D, Dong Y, Hu BH (2014) Molecular profile of cochlear immunity in the resident cells of the organ of Corti. J Neuroinflammation 11:173.

Chen L, Guo W, Ren L, Yang M, Zhao Y, Guo Z, Yi H, Li M, Hu Y, Long X, Sun B, Li J, Zhai S, Zhang T, Tian S, Meng Q, Yu N, Zhu D, Tang G, Tang Q, et al. (2016) A de novo silencer causes elimination of MITF-M expression and profound hearing loss in pigs. BMC Biol 14:52.

Chen W, Hao QQ, Ren LL, Ren W, Lin HS, Guo WW, Yang SM (2018) Cochlear morphology in the developing inner ear of the porcine model of spontaneous deafness. BMC Neurosci 19:28.

Chen Z, Wang F, Fei JI, Yang S, Nan WU (2016) Characteristics of auditory brainstem responses in miniature pigs and changes after impulse noise exposure. Chin J Otol 14:735-739.

Chen ZT. Research of inner ear delivery based on mPEG-PLGA nanocarrier for protein. Beijing: Chinese PLA Medical School 2014.

Dostert C, Pétrilli V, Van Bruggen R, Steele C, Mossman BT, Tschopp J (2008) Innate immune activation through Nalp3 inflammasome sensing of asbestos and silica. Science 320:674-677.

Duewell P, Kono H, Rayner KJ, Sirois CM, Vladimer G, Bauernfeind FG, Abela GS, Franchi L, et al. (2010), NLRP3 inflammasomes are required for atherogenesis and activated by cholesterol crystals. Nature 464:1357-1361.

Duewell P, Kono H, Rayner KJ, Sirois CM, Vladimer G, Bauernfeind FG, Abela GS, Franchi L, Nuñez G, Schnurr M, Espevik T, Lien E, Fitzgerald KA, Rock KL, Moore KJ, Wright SD, Hornung V, Latz E (2010) NLRP3 inflammasomes are required for atherogenesis and activated by cholesterol crystals. Nature 464:1357-1361.

Eisenbarth SC, Flavell RA (2009) Innate instruction of adaptive immunity revisited: the inflammasome. EMBO Mol Med 1:92-98.

Feng S, Yang L, Hui L, Luo Y, Du Z, Xiong W, Liu K, Jiang X (2020) Long-term exposure to low-intensity environmental noise aggravates age-related hearing loss via disruption of cochlear ribbon synapses. Am J Transl Res 12:3674-3687.

Frye MD, Ryan AF, Kurabi A (2019) Inflammation associated with noise-induced hearing loss. J Acoust Soc Am 146:4020.

Gross O, Thomas CJ, Guarda G, Tschopp J (2011) The inflammasome: an integrated view. Immunol Rev 243:136-151.

Hu BH, Cai Q, Hu Z, Patel M, Bard J, Jamison J, Coling D (2012) Metalloproteinases and their associated genes contribute to the functional integrity and noise-induced damage in the cochlear sensory epithelium. J Neurosci 32:14927-14941.

Hu BH, Zhang C, Frye MD (2018) Immune cells and non-immune cells with immune function in mammalian cochleae. Hear Res 362:14-24.

Koitschev A, Gramlich K, Hansmann S, Benseler S, Plontke SK, Koitschev C, Koetter I, Kuemmerle-Deschner JB (2012) Progressive familial hearing loss in Muckle-Wells syndrome. Acta Otolaryngol 132:756-762.

Kuemmerle-Deschner JB, Koitschev A, Tyrrell PN, Plontke SK, Deschner N, Hansmann S, Ummenhofer K, Lohse P, Koitschev C, Benseler SM (2015) Early detection of sensorineural hearing loss in Muckle-Wells-syndrome. Pediatr Rheumatol Online J 13:43.

Kurabi A, Keithley EM, Housley GD, Ryan AF, Wong AC (2017) Cellular mechanisms of noise-induced hearing loss. Hear Res 349:129-137.

Le TN, Straatman LV, Lea J, Westerberg B (2017) Current insights in noise-induced hearing loss: a literature review of the underlying mechanism, pathophysiology, asymmetry, and management options. J Otolaryngol Head Neck Surg 46:41.

Malik A, Kanneganti TD (2017) Inflammasome activation and assembly at a glance. J Cell Sci 130:3955-3963.

Marchica C, Zawawi F, Basodan D, Scuccimarri R, Daniel SJ (2018) Resolution of unilateral sensorineural hearing loss in a pediatric patient with a severe phenotype of Muckle-Wells syndrome treated with Anakinra: a case report and review of the literature. J Otolaryngol Head Neck Surg 47:9.

Martinon F, Burns K, Tschopp J (2002) The inflammasome: a molecular platform triggering activation of inflammatory caspases and processing of proIL-beta. Mol Cell 10:417-426.

Martinon F, Mayor A, Tschopp J (2009) The inflammasomes: guardians of the body. Annu Rev Immunol. 2009;27:229-265.

Nakanishi H, Kawashima Y, Kurima K, Chae JJ, Ross AM, Pinto-Patarroyo G, Patel SK, Muskett JA, Ratay JS, Chattaraj P, Park YH, Grevich S, Brewer CC, Hoa M, Kim HJ, Butman JA, Broderick L, Hoffman HM, Aksentijevich I, Kastner DL, et al. (2017) NLRP3 mutation and cochlear autoinflammation cause syndromic and nonsyndromic hearing loss DFNA34 responsive to anakinra therapy. Proc Natl Acad Sci U S A 114:E7766-7775.

Percie du Sert N, Hurst V, Ahluwalia A, Alam S, Avey MT, Baker M, Browne WJ, Clark A, Cuthill IC, Dirnagl U, Emerson M, Garner P, Holgate ST, Howells DW, Karp NA, Lazic SE, Lidster K, MacCallum CJ, Macleod M, Pearl EJ, et al. (2020) The ARRIVE guidelines 2.0: Updated guidelines for reporting animal research. PLoS Biol 18:e3000410.

Sai N, Shi X, Zhang Y, Jiang QQ, Ji F, Yuan SL, Sun W, Guo WW, Yang SM, Han WJ (2020) Involvement of cholesterol metabolic pathways in recovery from noise-induced hearing loss. Neural Plast 2020:6235948.

Schneider CA, Rasband WS, Eliceiri KW (2012) NIH Image to ImageJ: 25 years of image analysis. Nat Methods 9:671-675.

Schroder K, Tschopp J (2010) The inflammasomes. Cell 140:821-832.

Shi X, Dong Y, Li Y, Zhao Z, Li H, Qiu S, Li Y, Guo W, Qiao Y (2015) Inflammasome activation in mouse inner ear in response to MCMV induced hearing loss. J Otol 10:143-149.

Shi X, Qiu S, Zhuang W, Yuan N, Wang C, Zhang S, Sun T, Guo W, Gao F, Yang S, Qiao Y (2017) NLRP3-inflammasomes are triggered by age-related hearing loss in the inner ear of mice. Am J Transl Res 9:5611-5618.

Tran TA (2017) Muckle-Wells syndrome: clinical perspectives. Open Access Rheumatol 9:123-129.

Vethanayagam RR, Yang W, Dong Y, Hu BH (2016) Toll-like receptor 4 modulates the cochlear immune response to acoustic injury. Cell Death Dis 7:e2245.

Wang J, Puel JL (2018) Toward cochlear therapies. Physiol Rev 98:2477-2522.

Wang W, Zhang LS, Zinsmaier AK, Patterson G, Leptich EJ, Shoemaker SL, Yatskievych TA, Gibboni R, Pace E, Luo H, Zhang J, Yang S, Bao S (2019) Neuroinflammation mediates noise-induced synaptic imbalance and tinnitus in rodent models. PLoS Biol 17:e3000307.

Wu J, Han W, Chen X, Guo W, Liu K, Wang R, Zhang J, Sai N (2017) Matrix metalloproteinase-2 and -9 contribute to functional integrity and noise-induced damage to the blood-labyrinth-barrier. Mol Med Rep 1731-1738.

Yang S, Cai Q, Vethanayagam RR, Wang J, Yang W, Hu BH (2016) Immune defense is the primary function associated with the differentially expressed genes in the cochlea following acoustic trauma. Hear Res 333:283-294.

Yang SM (2016) The miniature pig as an animal model in otological research. Chin J Otol 14:1-5.

Zhang F, Dai M, Neng L, Zhang JH, Zhi Z, Fridberger A, Shi X (2013) Perivascular macrophage-like melanocyte responsiveness to acoustic trauma--a salient feature of strial barrier associated hearing loss. FASEB J 27:3730-3740.

Zheng F, Zuo J (2017) Cochlear hair cell regeneration after noise-induced hearing loss: Does regeneration follow development? Hear Res 349:182-196.

Zhong LL, Zhang Y, Liang XJ, Hou K, Han JW, Wang FY, Hao QQ, Jiang QQ, Yu N, Guo WW, Yang SM (2018) Inner ear structure of miniature pigs measured by multi-planar reconstruction techniques. Am J Transl Res 10:709-717.

Zhou R, Yazdi AS, Menu P, Tschopp J (2011) A role for mitochondria in NLRP3 inflammasome activation. Nature 469:221-225.

Zhuang W, Wang C, Shi X, Qiu S, Zhang S, Xu B, Chen M, Jiang W, Dong H, Qiao Y (2018) MCMV triggers ROS/NLRP3-associated inflammasome activation in the inner ear of mice and cultured spiral ganglion neurons, contributing to sensorineural hearing loss. Int J Mol Med 41:3448-3456.